CONFERENCE PRE-PRINT

OPTIMAL DESIGN OF FAST PLASMA BOUNDARY CONTROL CONSIDERING VERTICAL INSTABILITY FEATURES USING IN-VESSEL COILS IN JT-60SA

Shinichiro Kojima, Shizuo Inoue, Yoshiaki Miyata, Ko Yongtae, Hajime Urano, Takahiro Suzuki
National Institutes for Quantum Science and Technology
Naka, Ibaraki, Japan
Email: kojima.shinichiro@qst.go.jp

Abstract

Plasma shape plays a crucial role in determining plasma performance, and elongation in particular has a direct impact on fusion power and energy confinement time. However, conventional control methods do not allow direct specification of elongation and triangularity, since these parameters are determined from fixed control points together with the equilibrium of internal plasma pressure and current profiles. As a result, achieving high elongation and triangularity requires numerous trial-and-error adjustments and repeated discharges. To address this issue, we proposed the Dynamic Control Point (DCP) scheme for the plasma shape control, which sets the reference point near the last closed flux surface (LCFS). Although the DCP scheme enables direct control of elongation and triangularity, interference arises when it is combined with fast plasma position control using the in-vessel poloidal field coils. In this study, a Karush–Kuhn–Tucker (KKT) system is introduced to avoid control interference between the DCP scheme and fast plasma position control. Simulations with the MECS code demonstrated that a simple combination of DCP scheme and fast position control leads to interference and oscillations. In contrast, when the KKT system was applied in the fast position control, the interference was avoided, and stable coodinated operation was achieved. Through this approach, the controllable elongation during plasma current ramp-up was extended from $\kappa \sim 1.8$ to $\kappa \sim 2.05$, with high triangularity $\delta = 0.5$. The proposed method provides a general framework for coordinated control of superconducting coils and in-vessel coils, and applies not only to JT-60SA but also to other tokamak devices with different coil response times and control objectives.

1. INTRODUCTION

This study has developed a novel and stable plasma equilibrium control for high elongation ($\kappa > 2$) in a superconducting tokamak. High elongation plasma has many advantages in high performance plasma. The confinement time in H-mode scaling shows the relationship for elongation as $\kappa^{0.78}$ [1]. Furthermore, fusion power scales with elongation as κ^4 [2]. Increasing elongation provides significant economic benefits in nuclear fusion power plants. Controllability of plasma shaping is key to controlling the fusion power plant. However, high elongation can lead to a vertical displacement event (VDE) due to vertical instability. Vertical instability has been proven to be a kind of resistive wall mode (RWM) [3]. High-elongation plasmas always have a positive growth rate for vertical instability. This growth rate increases with higher levels of elongation. Therefore, fast feedback control is necessary for plasma shape/position control in order to achieve a high elongation level. In a superconducting tokamak, the response of the superconducting coil is slow. As the size of the tokamak device increases, the coil inductance also increases, causing larger devices to exhibit slower coil current response. To compensate for the slower coil current response due to superconducting coils, the in-vessel poloidal field coils (in-vessel coils) are/will be normally installed in superconducting tokamaks such as KSTAR [4], EAST [5], JT-60SA [6], ITER [7], DTT [8], CFETR [9], STEP [10]. In the JT-60SA experiment, a high level of elongation of 1.94 was achieved using in-vessel coils named fast plasma position control (FPPC) coils in a non-linear magnetohydrodynamic (MHD) simulation code MECS [11]. This elongation level was previously considered to be the limit with a lower SN configuration. A higher elongation level of > 2 could not be achieved. The elongation level is related to $nT\tau_E \propto \kappa^{7/2}$ [12]. If it were possible to increase the elongation level from 1.95 to 2.05, $nT\tau_E$ would increase by 20 %. The limitation of the elongation level should be increased to exceed 2. To achieve $\kappa > 2$, we reconsidered 1) the physics of vertical instability, and 2) the coordination of plasma equilibrium controls by superconducting and in-vessel coils. The first reconsideration concerns the location controlled by the in-vessel coils. In the general approach, the plasma shape and position are generally controlled by superconducting coils using the ISO-FLUX scheme, which adjusts the magnetic flux at the plasma boundary to match the magnetic flux at the X-point. In contrast, the conventional control by in-vessel

coils acts to reduce the vertical velocity of the plasma center. This mismatch in the controlled locations can lead to inconsistencies, and therefore, the control target of the in-vessel coils should be reconsidered based on the amplitude of vertical displacement by VDE. The second reconsideration is the coordinated control between the superconducting coils and the FPPC coils. Although control separation techniques have been developed in various devices to distinguish between the roles of superconducting coils and in-vessel coils, coordinated control by both systems is essential to reduce coil voltage and current demands and to avoid control interference. Based on these two reconsiderations, this study aims to achieve high-elongation plasmas with $\kappa > 2$ in a lower single-null configuration in JT-60SA.

2. SIMULATION OF VDE

The plasma equilibrium control in JT-60SA has been developed using the MECS code, which enables simulation of vertical displacement events (VDEs). The fast-moving region that should be controlled by in-vessel coils can be investigated with this code. The MECS code consists of two components: a plasma equilibrium solver and a plasma equilibrium controller. The controller, directly applicable to JT-60SA, is designed using magnetic reconstruction of the last closed flux surface (LCFS) based on the Cauchy Condition Surface (CCS) method. The solver self-consistently solves the Grad–Shafranov equation for the plasma current, eddy current, and prescribed internal parameters. It also simulates the time evolution of plasma equilibrium, including effects such as power supply dead time and sensor noise. Without any feedback coil current, elongated plasmas naturally move vertically as a VDE. The plasma displacement in the R–Z plane, obtained from solving the Grad–Shafranov equation, can be analyzed to identify the control target for vertical instability. The vertical displacement ΔZ with growth rate γ and amplitude δZ of VDE is described as $\Delta Z = \delta Z e^{\gamma t}$. Using fitting for the exponential growth rate and amplitude, we investigated the feature of vertical instability for various elongation levels in the range of κ ~1.6 to 1.8, as shown in Fig. 1. ΔZ_a and ΔZ_0 describe the vertical displacement of the plasma boundary and plasma center. The higher elongation causes a larger vertical displacement. The plasma boundary displaces more than the plasma center, $\Delta Z_a > \Delta Z_0$. The increase in elongation causes a larger amplitude and a larger growth rate of VDE. The difference between the plasma boundary and the plasma center can be seen in the amplitude of the vertical instability. The amplitude of the plasma boundary is larger than that of the plasma center $\delta Z_a > \delta Z_0$. The difference between the plasma boundary and center becomes larger in higher elongation. In contrast, the growth rates between the plasma boundary and center are the same. It indicates that the single toroidal mode n=0 RWM is dominant in the VDE. Because of its larger displacement, even with the same growth rate, the plasma boundary exhibits faster motion than the plasma center. Therefore, the plasma boundary should be controlled to avoid the VDE, since its displacement is easier to detect. This tendency is stronger in higher elongation plasma. Accordingly, the fast plasma control by the in-vessel coils should be applied to the plasma boundary, rather than the general control, which is applied to the plasma center.

3. CONTROL METHOD

In JT-60SA, there are ten superconducting poloidal field coils, and there will be two FPPC coils as shown in Fig. 2. To approach the control of the plasma boundary by using FPPC coils, we applied the ISO-FLUX scheme [11] [13] . The ISO-FLUX scheme fixes the LCFS on the reference points by minimizing the magnetic flux difference of $\delta\boldsymbol{\psi}_S = \psi_{\text{surf.}} - \boldsymbol{\psi}_{\text{point}}$, where $\psi_{\text{surf.}}$ is the magnetic flux on the X-point or the limiter point, $\boldsymbol{\psi}_{\text{point}}$ is the magnetic fluxes on the reference points. In our approach [11] [13] , the reference points controlled by the in-vessel coils were two points. The closest points for FPPC coils were chosen. However, to increase the elongation level, the control points for the elongation and the triangularity should be arranged optimally. In the case of the DCP scheme, the closest points are far from FPPC coils and lose the information for the horizontal direction. Therefore, we newly chose the three reference points of P2, P28, and P13. The magnetic flux difference on P2 describes the horizontal displacement. The magnetic flux differences on P28, P13 describe the upper vertical displacement and the lower vertical displacement, respectively. The fast component of magnetic flux that can not be controlled by the superconducting coils is controlled by FPPC coils by the PD control with the frequency separation technique.

$$\delta\boldsymbol{\psi}_{\text{FP}} = G_{\text{P,FP}}\left(\delta\boldsymbol{\psi}_{\text{fast}} + T_{\text{D}}\frac{d\delta\boldsymbol{\psi}_{\text{cont.FP}}}{dt}\right), \tag{1}$$

where $\delta\boldsymbol{\psi}_{\text{FP}}$ represents the controlled magnetic fluxes by the FPPC coils, $G_{\text{P,FP}}$ and T_{D} represent the proportional gain and the derivative coefficient, $\delta\boldsymbol{\psi}_{\text{cont.FP}}$ represents the magnetic flux differences on P2, P28, and P13, $\delta\boldsymbol{\psi}_{\text{fast}}$ represents the high-frequency elements of $\delta\boldsymbol{\psi}_{\text{cont.FP}}$. The high-frequency element is extracted by using the finite impulse response filter, which has a cut-off frequency higher than the controlled frequency by superconducting coils. The FPPC coils are connected to individual power supplies. It is possible to individually change the coil

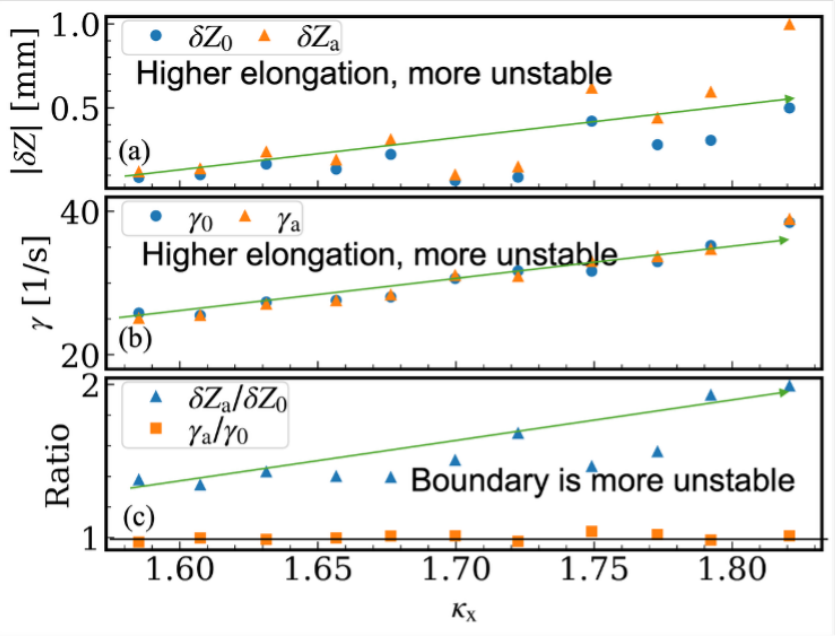

FIG. 1. (a) The coefficient and (b) the growth rate of vertical instability on the plasma center and plasma boundary. "0" means the plasma center, and "a" means the plasma boundary in the subscript. (c) The ratio of those parameters between the plasma boundary and the plasma center versus the elongation level.

current change as $\delta \boldsymbol{I}_{\rm FP} = (\delta I_{\rm FPPC1}\ \delta I_{\rm FPPC2})^T$. The relation between magnetic flux changes and the FPPC coil current change can be described as $\delta \boldsymbol{\psi}_{\rm FP} = M_{\rm FP}\delta I_{\rm FP}$. However, the mutual inductance is $M_{\rm FP} \in \mathbb{R}^{3\times 2}$. To obtain the FPPC coil current change, the pseudo-inverse matrix $\boldsymbol{M}_{\rm FP}^{\dagger}$ by singular value decomposition (SVD) is applied as,

$$\delta \boldsymbol{I}_{\rm FP} = \boldsymbol{M}_{\rm FP}{}^{\dagger}\delta \boldsymbol{\psi}_{\rm FP}. \tag{2}$$

In contrast, the superconducting coils manage the plasma current and the plasma shape/position. The ISO-FLUX scheme is applied for the plasma current control. The magnetic flux differences of the plasma current for the reference plasma current as $\delta\psi_{\rm X} = -L_{\rm p}\left(I_{\rm p,ref} - I_{\rm p,mes}\right)$. The plasma shape/position control manages the magnetic flux differences on all control points as $\delta\boldsymbol{\psi}_{\rm cont.SC} = \psi_{\rm surf.} - \boldsymbol{\psi}_{\rm cont.}$. The controlled magnetic flux by superconducting coils for the plasma current is given by the PID control as

$$\delta\psi_{\rm X,cont.} = G_{X,\rm AVA}\left(G_{\rm PX}\,\delta\psi_X + G_{\rm IX}\int \delta\psi_X\,dt + G_{\rm DX}\frac{d\,\delta\psi_X}{dt}\right), \tag{3}$$

where $G_{\rm PX}$, $G_{\rm IX}$, and $G_{\rm DX}$ denote the proportional, integral, and derivative gains. The adaptive voltage allocation $G_{X,\rm AVA}$ represents the weighting applied to make a balance between the plasma shape/position control. As the same procedure, the controlled magnetic flux by superconducting coils for the plasma shape/position is given by the PID control as

$$\delta\boldsymbol{\psi}_{\rm S,cont.} = G_{\rm PS}\,\delta\boldsymbol{\psi}_{S,\rm SC} + G_{\rm IS}\int \delta\boldsymbol{\psi}_{S,\rm SC}\,dt + G_{\rm DS}\frac{d\,\delta\boldsymbol{\psi}_{S,\rm SC}}{dt}, \tag{4}$$

where $G_{\rm PS}$, $G_{\rm IS}$, and $G_{\rm DS}$ denote the proportional, integral, and derivative gains. $\boldsymbol{\psi}_{S,\rm SC} \in \mathbb{R}^{n\times 10}$, number of n depends on the imposed constraints. Since the number of control points increases with additional control points, $\boldsymbol{I}_{\rm SC}$ is determined by applying an appropriate inverse of the corresponding matrix (details are written in the latter) as,

$$\delta\boldsymbol{I}_{\rm SC} = \boldsymbol{M}_{\rm SC}{}^{\dagger}\left(\delta\psi_{\rm X,cont.} + \delta\boldsymbol{\psi}_{\rm S,cont.}\right) \tag{5}$$

Each coil current change can be described as $\delta\boldsymbol{I}_{\rm coil} = (\delta\boldsymbol{I}_{\rm SC}\ \delta\boldsymbol{I}_{\rm FP})^T$. The applied command voltage is given as,

$$\boldsymbol{V}_{\rm com} = \boldsymbol{M}_{\rm coil}\frac{d\boldsymbol{I}_{\rm coil}}{dt} + \frac{d}{dt}\left(\boldsymbol{M}_{\rm pl}\,I_p\right), \tag{6}$$

where $\boldsymbol{V}_{\mathrm{com}}$ denotes the command voltage vector, $\boldsymbol{M}_{\mathrm{coil}}$ denotes a two-dimensional matrix whose diagonal/off-diagonal elements are of self/mutual inductance for coils, $\boldsymbol{M}_{\mathrm{pl}}$ denotes the mutual inductance vector between the coils and the plasma, assuming the filament current on the plasma current center. Note that the voltage for resistive loss is not applied to reduce the FPPC coil current due to the resistive loss.

In the previous approach, control points were pre-programed as time-depedent values to design the desired plasma formation[11]. Such a pre-programmed control point method is the conventional practice in devices employing the ISO-FLUX scheme. However, it requires numerous trials and adjustments to arrange the control point locations. Even if several LCFS points are fixed at control points, the plasma formation still depends on the internal plasma parameters β_{p} and l_{i}, making it impossible to maintain elongation and triangularity. To overcome this issue, we proposed a new plasma shape/position control for setting the control point locations by the Dynamic Control Point (DCP) scheme based on plasma elongation and triangularity [14]. We here define its implementation as a plasma shape/position control by superconducting coils, referred to as DCP control. In the DCP control, the major radius of the innermost P4 and the outermost P2 points is prescribed, while their vertical positions are determined by the innermost and outermost points of the LCFS, respectively. In addition, the upper control points are defined from the uppermost point of the LCFS. The uppermost point is identified at first, then a circle with a prescribed radius is drawn with this point as its center, and its intersections with the LCFS are obtained. The upper control points, P27 and P28, are then defined as shifted intersections, with the shift calculated from the reference uppermost point. In this study, we adopt a six-point configuration essential for controlling elongation and triangularity. It should be emphasized that conventional control maintains the LCFS using pre-programmed control points, whereas DCP control must manage the LCFS using active control points that change dynamically with the LCFS. This is potentially challenging, since the control points themselves move as the LCFS moves. This study represents the first attempt to combine fast position control by the FPPC coils with the DCP control. It is reasonable to expect that such a combination induces control interference, because fast position control and DCP control both fix the LCFS on the control points, while the control points themselves move with the LCFS. Therefore, the fast position control influences the DCP control through movable control points, and vice versa. In this case, the control interference arises from structural coupling between the two controls, which cannot be avoided by frequency separation alone. If a method can be established to combine both controls without interference by taking their mutual influence into account, higher elongation and triangularity can be maintained. Moreover, at high elongation, the plasma tends to form a double-null (DN) configuration. However, the upper divertor has a much lower heat-flux handling capability than the lower divertor: it can withstand only about 0.1 MW/m^2 for 100 s, whereas the lower divertor plate can handle up to 1 MW/m^2 for 100 s using carbon armor tiles bolted on water-cooled copper alloy (and up to 10 MW/m^2 for 100 s with brazed CFC monoblocks). Because of this limitation, the plasma must be prevented from striking the upper divertor. To avoid this, we developed a null control logic, which is a scheme for plasma shape and position control using superconducting coils. A detailed discussion of the null control logic is beyond the scope of this paper; however, it is taken into account in the present simulation.

4. KARUSH–KUHN–TUCKER (KKT) SYSTEM

To avoid the control interference between the fast position control with FPPC coils and the DCP control with superconducting coils, the effect of the fast position control should be explicitly considered when computing the inverse of the corresponding matrix. For this purpose, the Karush–Kuhn–Tucker (KKT) system provides a suitable formulation to incorporate the FPPC coil contribution. By employing the KKT system, the constrained least squares problem can be solved. In this framework, while the FPPC coil current change is fixed for the fast position control, its influence on the plasma current control and plasma shape/position control can still be consistently taken into account. When considering plasma shape/position control, the fast position control by FPPC coil current change can be interpreted as controlling both the location of the last closed flux surface (LCFS) and the positions of the control points. Therefore, the KKT system provides a framework to mitigate control interference by explicitly accounting for the movement of control points. In this study, we applied the KKT system to the computation of the matrix inverse. The KKT system is derived from the Lagrangian function with the constrained least squares problem as

$$\mathcal{L} = \|\delta\boldsymbol{\psi} - \boldsymbol{M}_{\mathrm{coil}}\delta\boldsymbol{I}_{\mathrm{coil}}\|^2 + \lambda \|\delta\boldsymbol{I}_{\mathrm{coil}}\|^2 + \Lambda^{\mathrm{T}} \left(\boldsymbol{C}\,\delta\boldsymbol{I}_{\mathrm{coil}} - \delta\boldsymbol{I}_{\mathrm{FP}}\right), \tag{7}$$

where $\mathcal{L}$ denotes the Lagrangian, $\delta\boldsymbol{\psi}$ denotes the controlled magnetic flux difference, λ denotes the weight of the Tikhonov regularization, Λ denotes the Lagrange multipliers corresponding to the equality constraints. $\boldsymbol{C}$ denotes the matrix used to impose the fixed coil current constraints. The matrix structure is $\boldsymbol{C} \in \mathbb{R}^{12\times 2}$. To impose the constraint of fixing the FPPC coil current change, the selection matrix is constructed with nonzero entries at $\boldsymbol{C}_{11,1}$ = 1, $\boldsymbol{C}_{12,2}$ =1, while all other entries are set to zero. $\delta\boldsymbol{I}_{\mathrm{FP}}$ denotes the FPPC coil current based on the fast position control. By satisfying the following condition, the constrained least squares problem can be solved while fixing

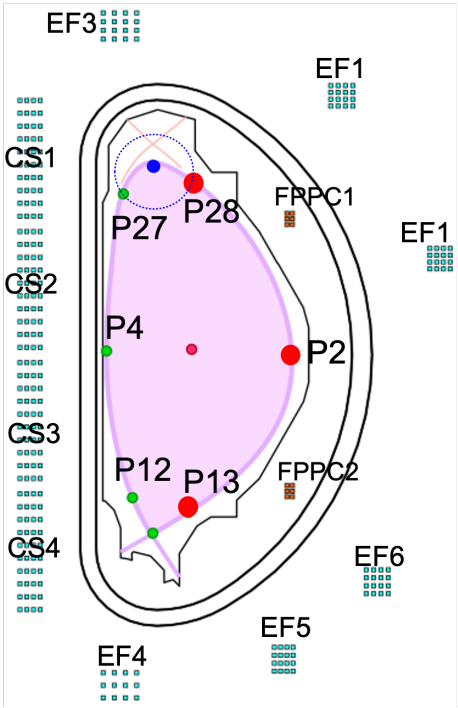

FIG. 2. Plasma shape change with high elongation in the MECS code. The arrangements of control points used in the DCP control are shown in a poloidal cross-section. The red points of P28, P2, and P13 denote the control points controlled by superconducting coils and FPPC coils. The green points of P27, P4, and P12 denote the control points controlled by the superconducting coils only. The arrangements of ten superconducting poloidal field coils and two FPPC coils are shown. Four center solenoid (CS) coils and six equilibrium field (EF) coils are equipped as superconducting poloidal field coils.

the FPPC coil current as

$$\frac{\partial \mathcal{L}}{\partial\, \delta \boldsymbol{I}_{\rm coil}} = \left(2\boldsymbol{M}_{\rm coil}^{\rm T}\boldsymbol{M}_{\rm coil} + 2\lambda \boldsymbol{E}\right)\delta \boldsymbol{I}_{\rm coil} - 2\boldsymbol{M}_{\rm coil}^{\rm T}\delta\boldsymbol{\psi} + \boldsymbol{C}^{\rm T}\Lambda = 0, \tag{8}$$

$$\frac{\partial \mathcal{L}}{\partial \Lambda} = \boldsymbol{C}\,\delta \boldsymbol{I}_{\rm coil} - \delta \boldsymbol{I}_{\rm FP} = 0. \tag{9}$$

These conditions indicate that, for a convex system, the Lagrangian is minimized with respect to all coil current changes while ensuring the FPPC coil current change can be fixed at the prescribed value for the fast position control. It can be summarized to the KKT system as

$$\begin{bmatrix} 2\boldsymbol{M}_{\rm coil}^{\rm T}\boldsymbol{M}_{\rm coil} + 2\lambda\boldsymbol{E} & \boldsymbol{C}^{\rm T} \\ \boldsymbol{C} & \boldsymbol{0} \end{bmatrix} \begin{bmatrix} \delta\boldsymbol{I}_{\rm coil} \\ \Lambda \end{bmatrix} = \begin{bmatrix} 2\boldsymbol{M}_{\rm coil}^{\rm T}\delta\boldsymbol{\psi} \\ \delta\boldsymbol{I}_{\rm FP} \end{bmatrix}. \tag{10}$$

This KKT system can be modified to the same form applied in Eq.2. The overall coil current change can instead be expressed as

$$\delta \boldsymbol{I}_{\rm coil} = \boldsymbol{M}_{\rm KKT}^{\dagger}\,\delta\boldsymbol{\psi} + \boldsymbol{C}_{\rm cons}\,\delta\boldsymbol{I}_{\rm FP}, \tag{11}$$

where $\boldsymbol{M}_{\rm KKT}^{\dagger}$ denotes a pseudo-inverse matrix constructed to satisfy the KKT system, and $\boldsymbol{C}_{\rm cons}$ denotes the correction matrix used to fix the FPPC coil current change. The quantity $\delta\boldsymbol{\psi}$ can be chosen as $\delta\psi_{\rm X,cont.}$ for plasma current control only, $\delta\boldsymbol{\psi}_{\rm S,cont.}$ for plasma shape/position control only, or $\left(\delta\psi_{\rm X,cont.} + \delta\boldsymbol{\psi}_{\rm S,cont.}\right)$ when both are controlled. Accordingly, this inverse matrix can be applied to determine the adaptive voltage allocation gains. From this formulation derived from the KKT system, provided that the FPPC coil current change does not interfere with the DCP control by the superconducting coils, the FPPC coils can coordinate with the DCP control and simultaneously contribute to plasma current and shape/position control. Therefore, there is no potential control interference with the control performed by the FPPC coils. This concept can be clarified by the explicit forms of $\boldsymbol{M}_{\rm KKT}^{\dagger}$ and $\boldsymbol{C}_{\rm cons}$, given as

$$\boldsymbol{H} = 2\boldsymbol{M}_{\rm coil}^{\rm T}\boldsymbol{M}_{\rm coil} + 2\lambda\boldsymbol{E}, \tag{12}$$

$$\boldsymbol{C}_{\mathrm{cons}} = \boldsymbol{H}^{-1}\boldsymbol{C}^{\mathrm{T}}\left(\boldsymbol{C}\boldsymbol{H}^{-1}\boldsymbol{C}^{\mathrm{T}}\right)^{-1}, \tag{13}$$

$$\boldsymbol{M}^{\dagger}_{\mathrm{KKT}} = \left(\boldsymbol{H}^{-1} - \boldsymbol{C}_{\mathrm{cons}}\boldsymbol{C}\boldsymbol{H}^{-1}\right)2\boldsymbol{M}^{\mathrm{T}}_{\mathrm{coil}}. \tag{14}$$

As shown in the above equations, part of $\boldsymbol{M}^{\dagger}_{\mathrm{KKT}}$ cancels out the effect of the fixed FPPC coil current change. Therefore, the FPPC coil current change prescribed by the fast position control can be incorporated consistently without interruption for the plasma current and shape/control by superconducting coils.

5. DCP CONTROL WITH KKT SYSTEM

A comparison between a simple combination of DCP control with fast position control and the combination with the KKT system is shown in Fig. 3. The scenario simulates plasma ramp-up with 6 MW NBI heating starting from 2.5 s (see (a)), and the prescribed poloidal beta and internal inductance are set accordingly (see (b)). During the ramp-up, the target plasma shaping in terms of elongation and triangularity is satisfied (see (c, d)). However, as initially expected, control interference occurs and leads to a VDE during the ramp-up. Oscillations appear in the vertical position of control point P2 (see (e)), indicating that the LCFS itself is oscillating. The vertical oscillation is particularly pronounced just before the VDE (see (h)), and oscillations are also observed in the superconducting coil currents (see (i)) as well as in the FPPC coil currents (see (j)). Consequently, the magnetic flux difference between the control point and the LCFS fails to converge and continues to oscillate, resulting in degraded control performance. In contrast, when DCP control is combined with fast position control using the KKT system, control interference is successfully avoided, again as initially expected, and stable control is achieved. As a result, high elongation with $\kappa \approx 2$ is obtained. In particular, the vertical oscillation of control point P2 is suspended (see (h)), and no oscillations are observed in either the superconducting coil currents (see (i)) or the FPPC coil currents (see (j)). Consequently, the magnetic flux difference between the control point and the LCFS is well controlled, the fast position control effectively contributes to plasma shape and position control, and excellent performance is achieved in reaching the reference elongation. It should be emphasized that the difference between the two cases arises solely from the use or non-use of the KKT system. The KKT system is thus essential when incorporating both fast plasma position control and DCP control.

In the DCP control, both elongation and triangularity can be referenced even during plasma ramp-up, when internal parameters such as the pressure and current profiles change significantly. Here, the same internal parameters as in Fig. 3 are adopted, and the operational region for elongation and upper triangularity is investigated. For a fair comparison, the lower X-point and the lower triangularity are fixed. As shown in Fig. 4, in the simple combination of DCP control with fast position control, the achievable elongation κ is limited to approximately 1.9. This value is close to the JT-60SA design target and satisfies the elongation range achieved in previous studies [11]. However, further increase in elongation is not possible because control interference arises. Unless the vertical instability property is improved, elongation cannot be increased beyond this limit. For example, it can be enhanced by bringing the plasma closer to the wall at an upper triangularity of $\delta_u \approx 0.3$. In contrast, DCP control combined with fast position control using the KKT system significantly expands the operational region, achieving a maximum elongation of $\kappa \approx 2.05$ with upper triangularity ranging from $\delta_u \approx 0.3$ to $\delta_u \approx 0.6$. This not only exceeds the JT-60SA design target for elongation but also enables stable controllability across a wide range of triangularities. These results demonstrate that high-elongation, high-triangularity plasmas can be referenced arbitrarily.

6. SUMMARY

The plasma shape significantly contributes to plasma performance, and in particular, elongation is known to directly affect fusion power and the energy confinement time. However, control schemes that allow direct specification of elongation are limited. In many existing control methods, elongation and triangularity are determined from the prescribed control points together with the equilibrium of internal plasma pressure and current profiles. As a result, achieving arbitrary values of elongation and triangularity requires numerous trial-and-error adjustments and many discharges. To address this issue, previous studies established a plasma shape control based on a Dynamic Control Point (DCP) scheme, in which the control points are set with reference to the last closed flux surface (LCFS). Here, the plasma shape/position control by superconducting coils is referred to as the DCP control. This enables specification of the control point positions based directly on elongation and triangularity. In this study, the DCP control was employed with the aim of achieving high-elongation plasmas ($\kappa > 2$). The control approach using the in-vessel poloidal coils, named FPPC coils, was reconsidered in terms of the controlled locations, and

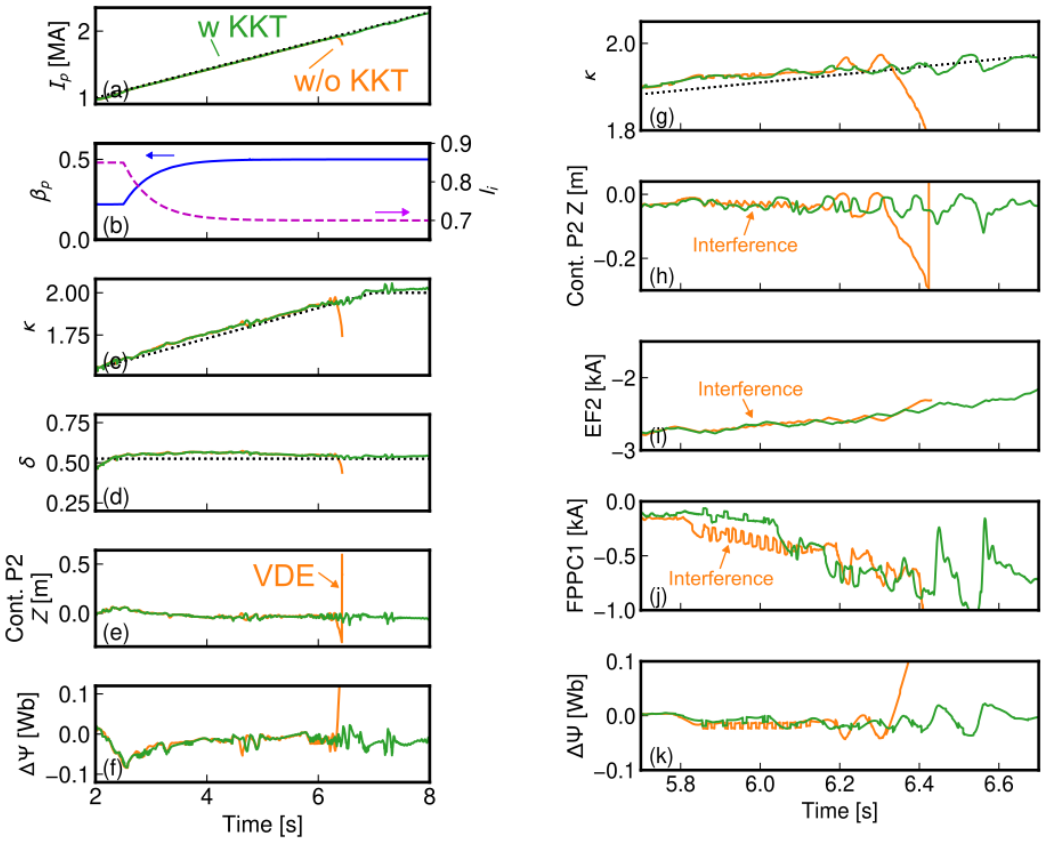

FIG. 3. Time evolution of (a) plasma current, (b) poloidal beta and internal inductance, (c) elongation, (d) triangularity, (e) vertical location of control point P2, and (f) averaged flux difference used for shape control. Panels (g)–(k) present enlarged views around the time of the vertical displacement event (VDE) in the case without the KKT system: (g) elongation, (h) vertical location of control point P2, (i) EF2 coil current, (j) FPPC1 coil current, and (k) averaged flux difference used for shape control. The simple combination of DCP control with fast position control results in vertical oscillations due to control interference. In contrast, the combination of both with the KKT system avoids such interference.

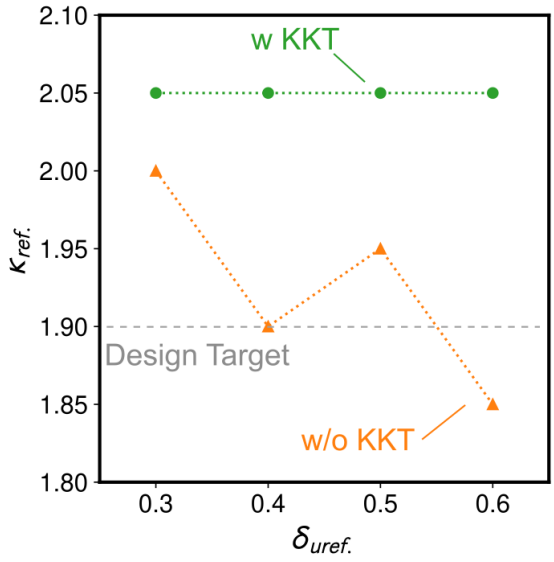

FIG. 4. Operational region for the reference elongation and triangularity obtained with DCP control and fast position control by the FPPC coils without/with the KKT system during plasma current ramp-up (ramp-up rate of 214 kA/s). The controllable elongation improves to $\kappa = 2.05$ with a wide triangularity from $\delta = 0.3$ to $\delta = 0.5$ by the coordinated control of the KKT system.

coordinated operation of the fast plasma position control by the FPPC coils and the DCP control was investigated. First, focusing on the characteristics of vertical instability, the VDE was reproduced in the MECS code, and the displacements of both the plasma boundary and the plasma center were evaluated. The results showed that the plasma boundary has larger displacement than the plasma center, that the amplitude of vertical instability is larger at the plasma boundary, and that this difference becomes greater as the elongation increases. These findings indicate that suppression of vertical instability is more effective when controlling the plasma boundary. Therefore, the ISO-FLUX scheme was adopted for the fast plasma position control by FPPC coils, in order to control the plasma boundary. However, there is potential for control interference between the two controls. Next, coordinated control of the two controls using the Karush–Kuhn–Tucker (KKT) system was introduced. The KKT system enables DCP control to be performed independently of the fixed FPPC coil current changes used for the fast position control. By applying the KKT system, the control interference between the two controls can be avoided. Simulations with the MECS code demonstrated that simply combining DCP control with fast position control by FPPC coils leads to control interference and oscillations. In contrast, using the KKT system, the control interference was avoided, and stable coordinated operation was achieved. Through this coordinated operation, it was shown that, whereas the maximum controllable elongation during plasma current ramp-up with DCP control without the KKT system was about $\kappa \approx 1.9$ with a triangularity of $\delta \approx 0.4$–0.6, the inclusion of fast plasma position control with the KKT system enabled elongation of $\kappa = 2.05$ and triangularity of $\delta = 0.3$–0.6. This result demonstrates that the proposed approach, which employs the KKT system to eliminate potential for control interference between the control by superconducting coils and the control by FPPC coils, enables stable coordinated control. The proposed scheme using the KKT system is not limited to JT-60SA but can be applied to a wide range of tokamak devices with different coil response times and control objectives, and it contributes to the realization of high-performance plasma operation.

ACKNOWLEDGEMENTS

JT-60SA was jointly constructed and is jointly funded and exploited under the Broader Approach Agreement between Japan and EURATOM.

REFERENCES

[1] ITER PHYSICS EXPERT GROUPS ON CONFINEMENT AND TRASPORT AND CONFINEMENT MODELLING AND DATABASE, Chapter 2 : Plasma confinement and transport ITER physics expert groups on confinement and transport and confinement modelling and database, Nucl. Fusion **39** 12 (1999).

[2] MENARD, J. E. et al., Fusion nuclear science facilities and pilot plants based on the spherical tokamak, Nucl. Fusion **56** 10 (2016) 106023.

[3] FREIDBERG, J. P. et al., Tokamak elongation – how much is too much? part 1. theory, J. Plasma Phys. **81** 6 (2015).

[4] KIM H K, YANG H L, KIM G H, KIM J, JHANG H, BAK J S AND LEE G S, Design features of the KSTAR in-vessel control coils, Fusion Eng. Des. **84** 2-6 (2009) 1029–1032.

[5] YAO, D. et al., Overview of the EAST in-vessel components upgrade, Fusion Eng. Des. **98-99** (2015) 1692–1695.

[6] ASAKAWA, S. et al., Design of the fast plasma position control coils for JT-60SA, `http://www.jspf.or.jp/JPFRS/PDF/Vol9/jpfrs2010_09-226.pdf`, Accessed: 2022-1-5.

[7] NEUMEYER, C. et al., Design of the ITER in-vessel coils, Fusion Sci. Technol. **60** 1 (2011) 95–99.

[8] AMBROSINO, R. et al., Conceptual design of the DTT in-vessel equatorial coils, Fusion Eng. Des. **194** (2023) 113714.

[9] LIU, L. et al., Concept design and analysis of CFETR vertical instability control using passive plates and in-vessel coils, J. Fusion Energy **34** 5 (2015) 1129–1133.

[10] ANAND, H. et al., Modelling, design and simulation of plasma magnetic control for the spherical tokamak for energy production (STEP), Fusion Eng. Des. **194** 113724 (2023) 113724.

[11] KOJIMA, S. et al., Effects of non-rigidity on fast plasma boundary control using in-vessel coils in JT-60SA, Nucl. Fusion **65** 8 (2025) 086003.

[12] COSTLEY, A. E., Towards a compact spherical tokamak fusion pilot plant, Philos. Trans. A Math. Phys. Eng. Sci. **377** 2141 (2019) 20170439.

[13] KOJIMA, S. et al., Development of controller for fast plasma position control coils with ISO-FLUX scheme on JT-60SA.

[14] INOUE, S. et al., Adaptive tikhonov regularization and dynamic control points for accurate shape parameter control of plasmas, Nucl. Fusion **64** 1 (2024) 016014.